

Technical report • May 2024

# Crystal Engineering for Water Treatment

Joy Ngozi Onwumere and Zhehao Huang

MISTRA  
**SAFE**CHEM 

### **A report from the Mistra SafeChem Programme**

Title: Development of Two-Dimensional Bismuth-Based Materials for Photocatalytic Degradation of Organic Molecules

Date: 2024-05-31

Deliverable number: D4.2.6

Contact person and email: Zehao Huang, [zehao.huang@mmk.su.se](mailto:zehao.huang@mmk.su.se)

### **About the authors**

Joy Ngozi Onwumere, inorganic chemistry, MMK, Stockholm University.

Zehao Huang Dr., inorganic chemistry, MMK, Stockholm University.

Mistra SafeChem is funded by Mistra (project number 2018/11).

Views and opinions expressed in this report are those of the authors only and do not necessarily reflect those of the entire Mistra SafeChem Programme or Mistra.

# Contents

Abstract .....	4
Introduction.....	5
Results and discussion.....	6
Conclusions.....	11
References.....	12
About Mistra SafeChem .....	13

## Abstract

Effective water pollution treatment is vital for protecting health, ecosystems, and supporting economic activities. Small organic pollutants, such as pesticides, pharmaceuticals, and industrial chemicals, persist in the environment and resist conventional methods, posing significant risks. Innovative catalysts are necessary for their effective degradation. Single-atom catalysts, with metal atoms dispersed on supports like metal oxides or carbon, offer exceptional activity and selectivity but tend to aggregate into clusters over time, and releasing into solutions as sub-micron particles. To address this, we developed a 2D crystalline catalyst through crystal engineering. Its 2D morphology and high surface area enhance efficiency in breaking down pollutants, while its micrometer size facilitates separation from water by precipitation, and avoid the risks posed by sub-micron particles. Using photodegradation, which harnesses light energy to decompose organic molecules, we demonstrate these catalysts can effectively degrade pollutants like Rhodamine B, showcasing their potential for advanced water treatment applications.

## Introduction

Water pollution treatment is essential for safeguarding human health, protecting ecosystems and supporting economic activities. Small organic molecules, including pesticides, pharmaceuticals, and industrial chemicals, are among the most pollutants in water. These pollutants are often resistant to conventional water treatment methods and can persist in the environment, leading to adverse effects on ecosystems and human health (Chong *et al.*, 2010). Therefore, it is urgent to develop novel catalysts which can provide high activity for degradation of such water pollutants.

Single-atom catalysts have recently been attracted intense interests as an advanced class of catalysts providing exceptional catalytic activity and selectivity. These catalysts, which are composed of individual metal atoms, are dispersed and stabilized on a support material, such as metal oxides or carbon (Wang, Li and Zhang, 2018). The atomic dispersion maximizes the utilization of metal atoms, and thus highly effective in water pollutant treatment. However, catalyst evolution during long-time reaction can lead to aggregation of the single-atoms. By forming metal clusters, they can be detached from the support materials, and release to the solution as sub-micron particles (Liu and Corma, 2018).

To tackle this challenge, we use crystal engineering approach and develop a 2D crystalline catalyst. As the catalyst exhibit a 2D morphology, it can effectively utilize its high surface area for providing high efficiency for water pollutant degradation. In addition, as the catalysts are in the size of several micrometres, we can effectively separate the catalysts from water by precipitation. By using photodegradation process, which uses light energy, e.g., from sunlight, to break down organic molecules, we demonstrate the catalysts can degrade Rhodamine B, which is an organic water pollutant. Compared to the benchmark  $\text{TiO}_2$  photocatalyst, our developed BiOBr nanosheet catalysts show high efficiency in photodegrading organic pollutants that are resistant to conventional treatment methods.

## Results and discussion

To design a catalyst that can effectively utilize solar energy and degrade organic compounds,  $\text{TiO}_2$  is the most researched material (Gopinath *et al.*, 2020) due to its low cost, non-toxicity, good chemical stability, (Hafeez *et al.*, 2022) and easy UV activation (Anucha *et al.*, 2022). However, the major drawback of  $\text{TiO}_2$  is that it has a band gap ( $\sim 3.2$  eV) too wide that it can only produce an optical response to ultraviolet light. (Arora *et al.*, 2022) Therefore, we explore bismuth-based compounds for water treatment due to their high photocatalytic activity (Ajiboye, Oyewo and Onwudiwe, 2021), stability, and electron mobility. (Kallawar, Barai and Bhanvase, 2021)

To synthesize the Bi composite, we used bismuth (III) bromide and titanium (IV) isopropoxide as the inorganic source, under solvothermal conditions. In addition, to control the growth of the catalyst for introducing high reactivity but remain a bulk material, not in a single-atom form, we added benzene-1,3,5-tricarboxylic acid during the synthesis. We obtained the product, BTO/BiOBr, which has a nanosheet morphology, and the aggregates are in the size of  $\sim 10$   $\mu\text{m}$ . For comparison, we synthesized BiOBr, which has an orthorhombic morphology with size of 2-8  $\mu\text{m}$  (Figure 1).

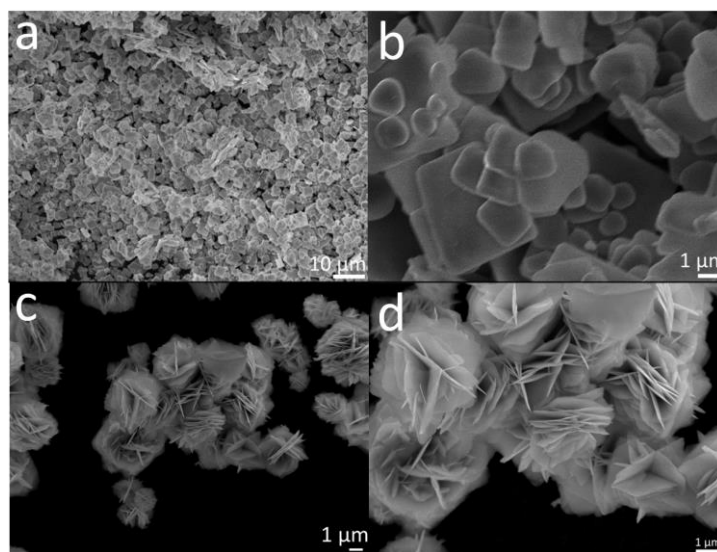


**Figure 1.** SEM images of (a and b) BiOBr and (c and d) BTO/BiOBr catalysts.

PXRD patterns of the synthesised BiOBr showed distinct peaks at c.a.  $11^\circ$ ,  $31.9^\circ$  and  $32.5^\circ$ , which attributed to the tetragonal BiOBr structure (JCPDS file No. 04-008-7926) (Figure 2). (Ketterer and Krämer, 1986) For the BTO/BiOBr, we found that its PXRD pattern is difficult to be indexed, as there are possible mixtures of tetragonal BiOBr (JCPDS file No. 01-085-0862), (Bannister, 1935) and orthorhombic  $\text{Bi}_4\text{Ti}_3\text{O}_{12}$  (JCPDS file No. 00-065-0233). (Roy *et al.*, 2011) Therefore, we used three-dimensional electron diffraction (3DED) to analyse the single crystal structure of the nanosheets (Table 1). From the reconstructed 3D reciprocal lattice (Figure 3a), the unit cell parameters can be determined as  $a = 4.19$  Å,  $b = 4.19$  Å,  $c = 8.41$  Å,  $\alpha = 87.89^\circ$ ,  $\beta = 88.89^\circ$ , and  $\gamma = 88.36^\circ$ . The crystal system could be tetragonal. The 2D slice cuts exhibited reflection condition as  $hk0: h + k = 2n$ ,  $0k0: k = 2n$  (Figures 3b-5d). Thus, the

possible space groups for BTO/BiOBr are  $P4/n$  (No. 85) and  $P4/nmm$  (No. 129). The 3DED data has a high signal-to-noise ratio within the resolution of  $0.80 \text{ \AA}$ , and the structure was successfully determined *ab initio* by direct methods using the space group  $P4/nmm$ . The final refinement converged to  $R1 = 0.284$  (Table 2). The structure determination shows a different structure from JCPDS file No. 04-008-7926 and 01-085-0862. Pawley fitting was performed to refine the unit cell parameters (Figure 4), which were refined to  $a = b = 3.9280(3) \text{ \AA}$ , and  $c = 8.128(1) \text{ \AA}$ . The R-values were converged to  $R_p = 0.031$ ,  $R_{wp} = 0.044$ , and  $R_{exp} = 0.012$ . To validate the structure, and analysis sample purity, we simulated a PXRD pattern using the structural model obtained from single crystal analysis and unit cell parameters refined by Pawley fitting (Figure 5). It exhibits a good match except the peak at c.a.  $7.1^\circ$ , which attributed to a minor impurity.

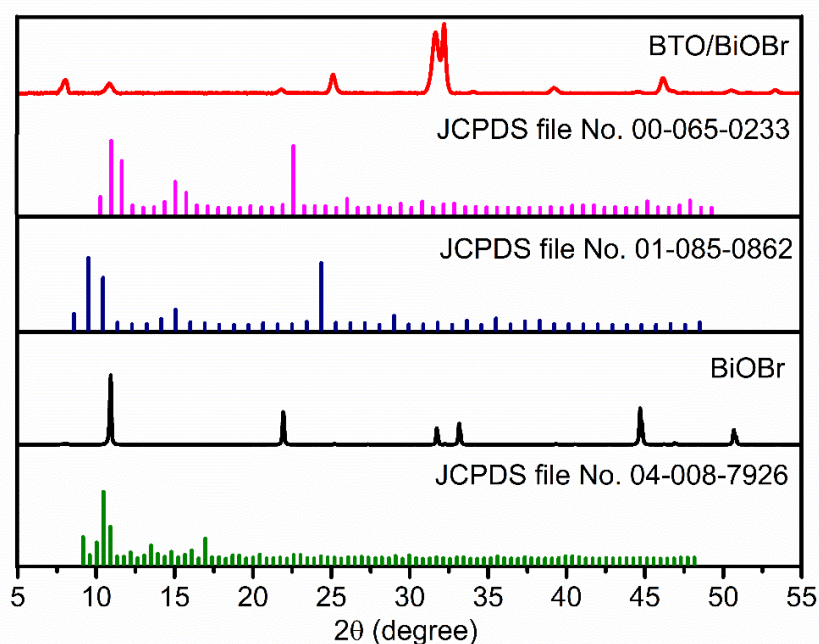


**Figure 2.** PXRD patterns of BTO/BiOBr, BiOBr and profiles from the JCPDS database.

**Table S1.** 3DED data collection for BiOBr ( $\lambda = 0.0251 \text{ \AA}$ ).

Tilt range ( $^\circ$ )	-53.0 to 61.3
Rotation angle ( $^\circ$ )	114.3
Tilt rate ( $^\circ \text{ s}^{-1}$ )	1.2
Exposure time per frame (s)	0.3
Total number of images	324
Data collection time (min)	1.6
Beam current (pA)	< 0.01

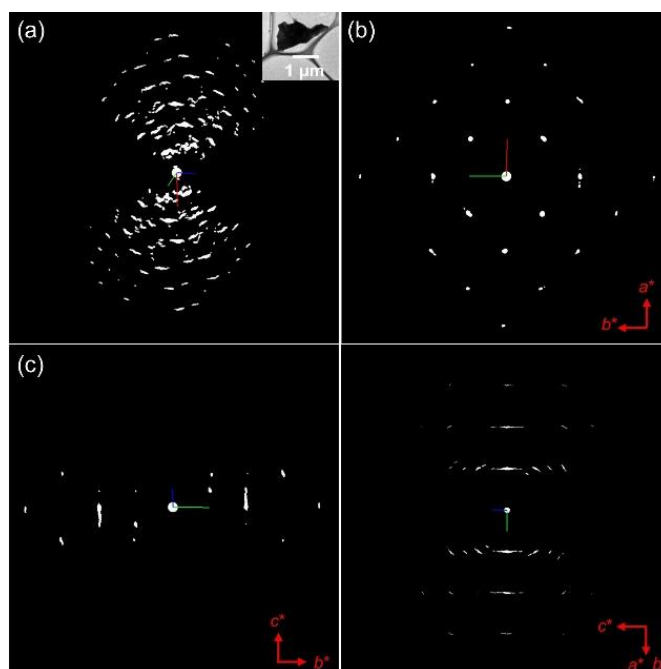


**Figure 3.** (a) The reconstructed 3D reciprocal lattice of BTO/BiOBr (an inset is an image of the crystal from which the 3DED data was collected) and 2D slice cuts show the (b)  $hk0$ , (c)  $0kl$ , and (d)  $hhl$  planes.

**Table 2.** Crystallographic details for BTO/BiOBr determined by 3DED ( $\lambda = 0.0251 \text{ \AA}$ ).

Chemical Formula	BiBrO
Formula weight	304.88
Crystal system	Tetragonal
Space Group	$P4/nmm$
$a$ ( $\text{\AA}$ )	4.1750(8)
$b$ ( $\text{\AA}$ )	4.1750(8)
$c$ ( $\text{\AA}$ )	8.570(2)
$\alpha$ ( $^\circ$ )	90
$\beta$ ( $^\circ$ )	90
$\gamma$ ( $^\circ$ )	90
Volume	149.38(6)
$Z$	2
Wavelength ( $\text{\AA}$ )	0.0251
Temperature (K)	293(2)
Completeness (%)	74.0
No. of reflections (all unique)	88
No. of reflections ( $F_o > 4\sigma(F_o)$ )	530
Refined parameters	6
$R_{\text{int}}$	0.2836
$R_1$ ( $F_o > 2\sigma(F_o)$ )	0.2571
$R_1$ (all reflections)	0.2635
GOF	3.458



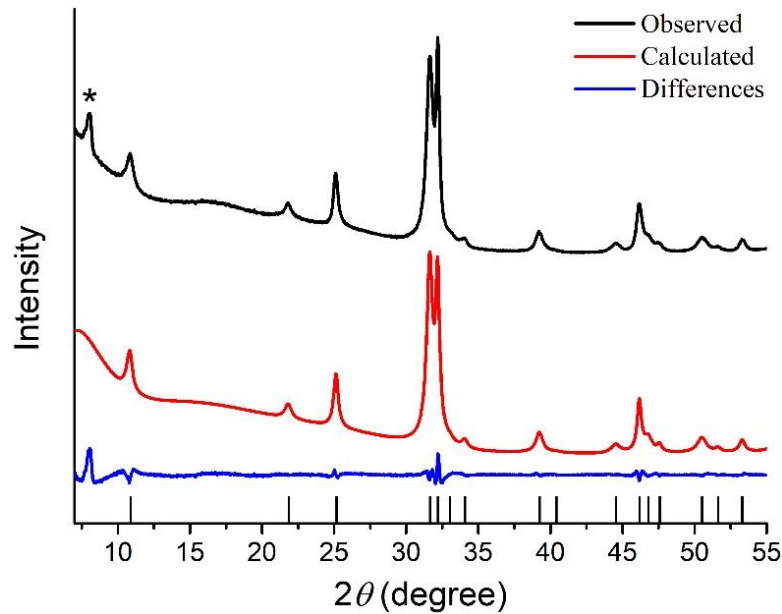


**Figure 4.** Pawley fitting against powder X-ray diffraction ( $\lambda = 1.5418\text{\AA}$ ) for BTO/BiOBr. Red line: calculated; black line: observed; blue line: difference; black bars: Bragg conditions. Asterisk indicates a minor impurity.

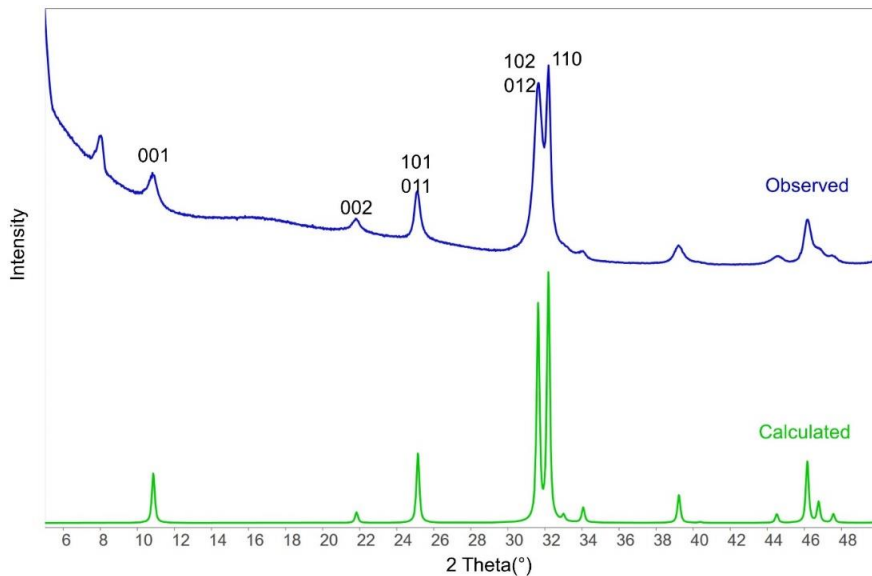


**Figure 5.** Simulated PXRD pattern ( $\lambda = 1.5418\text{\AA}$ ) of BiOBr by using the structural model obtained from 3DED. It agrees well with the observed PXRD pattern.

All catalysts, including BTO/BiOBr, and BiOBr and commercial  $\text{TiO}_2$  for comparison, showed excellent UV-Vis light absorption spectra, and the absorption band edges of BTO/BiOBr and BiOBr were extended beyond 400 nm. A Tauc plot is used to determine the optical bandgaps of BTO/BiOBr and BiOBr (Figure 6). The semiconductor energy band is calculated using the equation by intercepting the tangent lines according to the equation:

$$(\alpha h\nu)^{1/n} = A(h\nu - E_g) \quad (1)$$

where  $\alpha$  is absorption coefficient,  $h$  is Planck-constant,  $\nu$  is frequency,  $A$  is constant,  $E_g$  is the bandgap, respectively. As BTO/BiOBr, and BiOBr are indirect bandgap materials  $n = 2$ . Thus, the bandgaps of BiOBr and BTO/ BiOBr are determined as 2.95 and 3.03 eV, respectively (Figure 7), which are narrower compared to  $\text{TiO}_2$ , whose bandgap is  $\sim 3.2$  eV. (Guan *et al.*, 2023; Muthukrishnan, Vidya and Sjøstad, 2023)

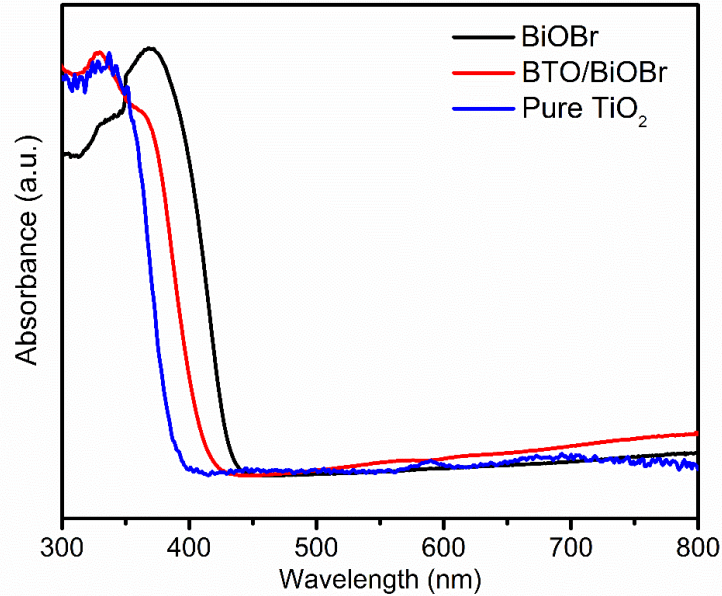


**Figure 6.** UV–Vis spectra of BiOBr BTO/BiOBr and  $\text{TiO}_2$ .

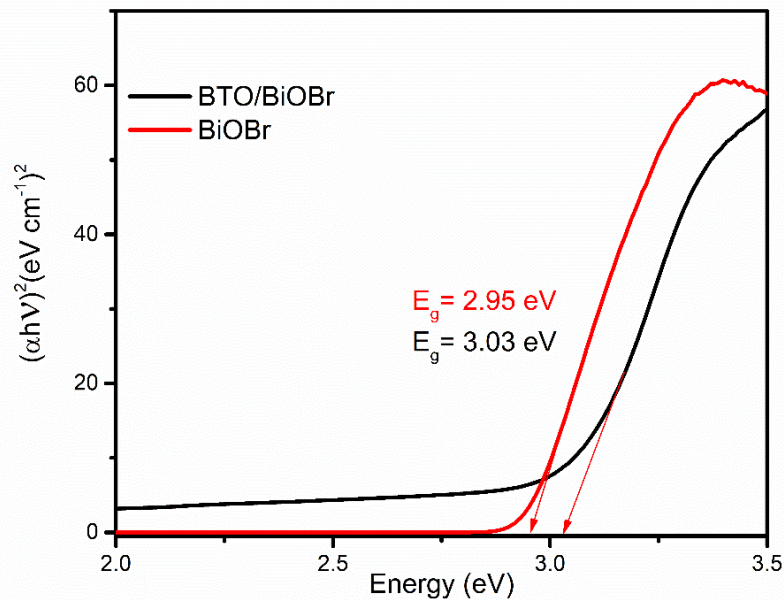


**Figure 7.** TAUC plot of BiOBr and BTO/BiOBr.

We demonstrate the efficiency of BTO/BiOBr nanosheets by using a test reaction to photocatalytically degrading RhB aqueous solution under simulated solar irradiation and compare its performance to those results obtained using conventional BiOBr and  $\text{TiO}_2$ . The RhB aqueous solution submerged in the catalysts was left in darkness for 20 minutes each to

reach adsorption equilibrium to remove the adsorption of RhB. The results were summarized in Figure 8. The photocatalytic degradation baseline is represented by the black and red curves with and without hydrogen peroxide ( $\text{H}_2\text{O}_2$ ), measured without a catalyst. The pure  $\text{TiO}_2$  and BiOBr showed a 55% and 36% degradation of the dye in solution, respectively, after 100 minutes. Compared to the single-phase catalyst, the BTO/BiOBr nanosheets performs much better, with about 100% degradation after 20 minutes.

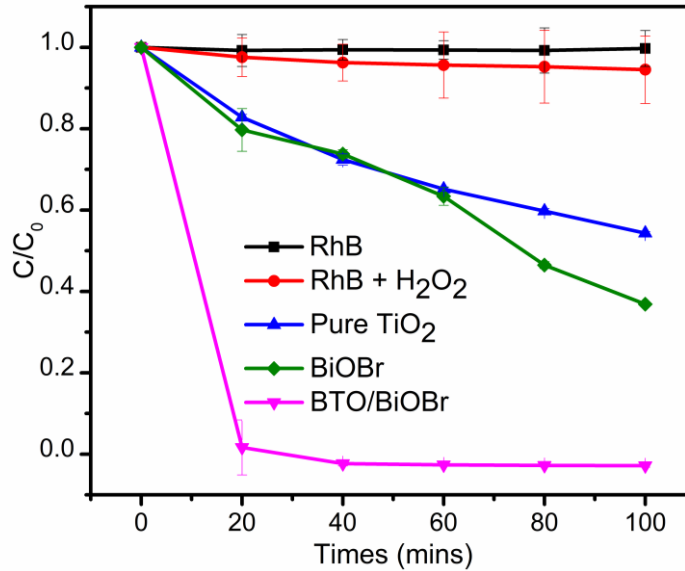


**Figure 8.** Photocatalytic degradation of RhB. Degradation was carried out using a solar simulator with hydrogen peroxide.

## Conclusions

In summary, we developed a novel BTO/BiOBr photocatalyst. By controlling the crystal growth, it has nanosheet morphology which provides ~5 times higher efficiency compared to benchmark material  $\text{TiO}_2$  and state-of-the-art material BiOBr. Moreover, the large particle size of BTO/BiOBr crystals can provide advantage in separating them from water. As a result, it can avoid second pollution of water by releasing sub-micron particles, which is common for highly efficient catalysts, such as single atom catalysts. Our approach provides a new way in balancing photocatalyst efficiency and its sustainability for water treatment.

## References

- Ajiboye, T.O., Oyewo, O.A. and Onwudiwe, D.C. (2021) ‘The performance of bismuth-based compounds in photocatalytic applications’, *Surfaces and Interfaces*, 23(January), p. 100927.
- Anucha, C.B. *et al.* (2022) ‘Titanium dioxide (TiO<sub>2</sub>)-based photocatalyst materials activity enhancement for contaminants of emerging concern (CECs) degradation: In the light of modification strategies’, *Chemical Engineering Journal Advances*, 10(September 2021), p. 100262.
- Arora, I. *et al.* (2022) ‘Advances in the strategies for enhancing the photocatalytic activity of TiO<sub>2</sub>: Conversion from UV-light active to visible-light active photocatalyst’, *Inorganic Chemistry Communications*, 143(June), p. 109700.
- Bannister, F.A. (1935) *THE MINERALOGICAL MAGAZINE AND JOURNAL OF THE MINERALOGICAL SOCIETY The crystal-structure of the bismuth oxyhalides.*
- Chong, M.N. *et al.* (2010) ‘Recent developments in photocatalytic water treatment technology: A review’, *Water Research*, 44(10), pp. 2997–3027.
- Gopinath, K.P. *et al.* (2020) ‘Present applications of titanium dioxide for the photocatalytic removal of pollutants from water: A review’, *Journal of Environmental Management*, 270(June), p. 110906.
- Guan, S. *et al.* (2023) ‘Oxygen vacancies induced band gap narrowing for efficient visible-light response in carbon-doped TiO<sub>2</sub>’, *Scientific Reports*, 13(1), pp. 1–9.
- Hafeez, M. *et al.* (2022) ‘Synthesis of cobalt and sulphur doped titanium dioxide photocatalysts for environmental applications’, *Journal of King Saud University - Science*, 34(4), p. 102028.
- Kallawar, G.A., Barai, D.P. and Bhanvase, B.A. (2021) ‘Bismuth titanate based photocatalysts for degradation of persistent organic compounds in wastewater: A comprehensive review on synthesis methods, performance as photocatalyst and challenges’, *Journal of Cleaner Production*, 318(July), p. 128563.
- Ketterer, J. and Krämer, V. (1986) ‘Structure refinement of bismuth oxide bromide, BiOBr’, *Acta Crystallographica Section C*, 42(8), pp. 1098–1099.
- Liu, L. and Corma, A. (2018) ‘Metal Catalysts for Heterogeneous Catalysis: From Single Atoms to Nanoclusters and Nanoparticles’, *Chemical Reviews*, 118(10), pp. 4981–5079.
- Muthukrishnan, S., Vidya, R. and Sjästad, A.O. (2023) ‘Band gap engineering of anatase TiO<sub>2</sub> by ambipolar doping: A first principles study’, *Materials Chemistry and Physics*, 299(January), p. 127467.
- Roy, M. *et al.* (2011) ‘Synthesis, structural and electrical properties of La and Nb modified Bi<sub>4</sub>Ti<sub>3</sub>O<sub>12</sub> ferroelectric ceramics’, *Journal of Physics and Chemistry of Solids*, 72(11), pp. 1347–1353.
- Wang, A., Li, J. and Zhang, T. (2018) ‘Heterogeneous single-atom catalysis’, *Nature Reviews Chemistry*, 2(6), pp. 65–81.

## About Mistra SafeChem

Mistra SafeChem is a research programme with the vision to enable and promote the expansion of a safe, sustainable, and green chemical industry.

The programme is developed with the twelve principles of green chemistry as a fundament.

The research combines the potential of innovative manufacturing processes, tools for hazard and risk screening, and life cycle assessment with ambitions and opportunities for the development and growth of a safe and sustainable chemical industry.

### **More information:**

News from the programme, publications, and persons to contact you find at the website

**[mistrasafechem.se](http://mistrasafechem.se)**

### **Programme host:**

IVL Swedish Environmental Research Institute



[www.mistrasafechem.se](http://www.mistrasafechem.se)

FUNDED BY

